

Theory of positronium formation with surface electrons for realistic band structures

Akira Ishii*

*Institute of Material Science, University of Tsukuba, Sakura-mura, Ibaraki 305, Japan
and Department of Physics, Waseda University, Okubo 3-4-1, Shinjuku-ku, Tokyo 160, Japan*

Shigeru Shindo

Department of Physics, Tokyo Gakugei University, Koganei, Tokyo 184, Japan

(Received 2 July 1986)

The energy and angular distributions of positroniums (Ps) formed at surfaces are calculated numerically using the integro-differential equation which appears in the dynamical theory of Ps formation based on the semiclassical trajectory approximation. The wide-band approximation, which is well known in the theory of neutralization of surface-scattered ions, is not adequate for the Ps formation. Strong deviation from the Born approximation is pointed out in the case of narrow-band electrons.

I. INTRODUCTION

Ps formation at metal surfaces is expected to be a sensitive probe for surface electronic structures. This comes from the fact that positron-electron bound states cannot be formed in the electron gas of realistic metals,¹⁻³ and Ps is therefore formed at the surfaces. From the theoretical point of view, Ps formation on surfaces can be compared with photoelectron emission. In the limit of the Born approximation,^{4,5} the Ps formation probability per unit time P becomes

$$P = \sum_{\mathbf{p}} \sum_{\mathbf{q}} \int dE_{\perp} \rho'(E_{\perp}) |W_{\mathbf{kq},\mathbf{p}}|^2 \delta(E_{\mathbf{k}} + E_{\mathbf{q}} - E_{\text{Ps}}(\mathbf{p})), \tag{1}$$

where E_{\perp} is the surface-normal electron energy, defined from surface-normal momentum k_{\perp} as $\sum_{k_{\perp}} = \int (dE_{\perp}/2\pi) \rho'(E_{\perp})$, where $\rho'(E_{\perp})$ is the one-dimensional density of states for surface electrons and $E = E_{\mathbf{k}} + E_{\mathbf{q}} - E_{\text{Ps}} - p^2/4$, where $E_{\mathbf{k}}$, $E_{\mathbf{q}}$, and $E_{\text{Ps}} + p^2/4$ are the energy of an electron with momentum \mathbf{k} , of a positron with momentum \mathbf{q} and of Ps with momentum \mathbf{p} , respectively. $W_{\mathbf{kq},\mathbf{p}}$ is the transition matrix element defined by Eq. (5) of this paper. The Ps energy is distributed between $p^2/4=0$ and $-\phi_{\text{Ps}}$, where ϕ_{Ps} is the work function of Ps, defined by

$$\phi_{\text{Ps}} = \phi_{+} + \phi_{-} - E_{\text{Ps}}, \tag{2}$$

where ϕ_{+} (ϕ_{-}) is the work function of the positron (electron). According to Eq. (1), the electron density of states of the outermost layer of the surface can be observed directly from the measurements of energy distributions.^{4,5} We name it "positronium formation spectroscopy (PsFS)". The schematic picture of PsFS is shown in Fig. 1. Since the formed Ps is a simple free particle in vacuum, the Ps distribution does not depend on the final electron density of states, in contrast to the photoelectron emission problem. This is one merit of PsFS for the

determination of the surface density of states in comparison with photoemission.

The Born approximation of Eq. (1) cannot be used for quantitative discussion because of normalization problems.⁵ Therefore, more detailed theories have been developed in recent years.⁵⁻⁹ Nevertheless, all of them utilize the wide-band approximation which was first introduced by Bloss and Hone¹⁰ in the theory of surface scattered-ion neutralization. Although the wide-band approximation has been confirmed as a powerful tool for ion neutralization,¹¹ nobody has investigated the validity of it in the case of positron neutralization or positronium formation. Moreover, the wide-band approximation cannot be applied to Ps formation in narrow bands, which is the case for transition metals. (Atomic units are used in this paper.)

Therefore, the purpose of this paper is to calculate Ps

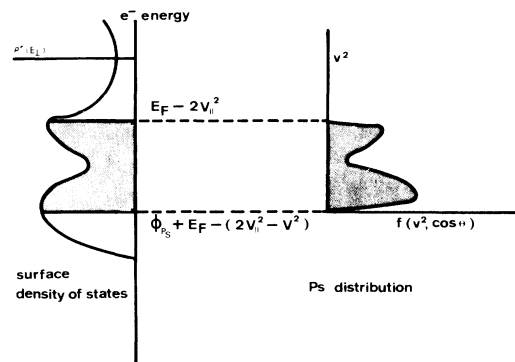


FIG. 1. Schematic picture of PsFS. The left graph is the one-dimensional density of states for surface electrons. The right graph is the corresponding Ps energy distribution. The lower limit and the upper limit of the Ps distribution is discussed in Sec. II. The distribution has a similar profile as that of the surface density of states. Here, v^2 is the kinetic energy of Ps in atomic units.

formation without the wide-band approximation, based on the semiclassical trajectory approximation. A numerical calculation is performed for the free-electron band and several narrow bands, using a calculation scheme similar to that of Sebastian and co-workers^{12,13} and Shindo and Kawai.¹¹

II. THEORY

Ps formation is described using the semiclassical trajectory approximation by the following coupled equations.⁶⁻⁸

$$i(d/dt)C_p(t) = \sum_{\mathbf{k}} V_{\mathbf{kq},\mathbf{p}}^* C_{\mathbf{k},\mathbf{q}}(t), \quad (3a)$$

$$i(d/dt)C_{\mathbf{k},\mathbf{q}}(t) = \sum_{\mathbf{p}} V_{\mathbf{kq},\mathbf{p}} C_p(t), \quad (3b)$$

where $C_p(t)$ is the amplitude of Ps with momentum \mathbf{p} , and $C_{\mathbf{k},\mathbf{q}}$ is that of the electron and the positron with mo-

menta \mathbf{k} and \mathbf{q} . $V_{\mathbf{kq},\mathbf{p}}$ is the transition matrix element of Ps formation defined by

$$V_{\mathbf{kq},\mathbf{p}} = \int d\mathbf{r}_+ \int d\mathbf{r}_- \psi_+^*(\mathbf{r}_+) \psi_-^*(\mathbf{r}_-) (1/|\mathbf{r}_+ - \mathbf{r}_-|) \times \psi_{\mathbf{p}_s}(\mathbf{r}_+, \mathbf{r}_-), \quad (4)$$

where ψ_+ , ψ_- , and $\psi_{\mathbf{p}_s}$ are the wave functions for the positron, the electron, and Ps, respectively.^{6,8} Since the momentum parallel to the surface is conserved because of the symmetry of the system, we can separate the matrix element into two parts as follows:

$$V_{\mathbf{kq},\mathbf{p}} = W_{\mathbf{kq},\mathbf{p}} \delta^2(\mathbf{p}_{\parallel} - \mathbf{k}_{\parallel} - \mathbf{q}_{\parallel}). \quad (5)$$

Equation (3a) represents the formation of Ps and Eq. (3b) corresponds to the dissociation of Ps into bulk electron and positron states. The surface states are not considered here. From Eqs. (3a), (3b), and (5) we obtain the following integro-differential equation:⁸

$$i \frac{d}{dt} C_p(t) = \sum_{k_{\perp}} W_{\mathbf{kq},\mathbf{p}}^* C_{\mathbf{k},\mathbf{q}}(t_0) - i \sum_{k_{\perp}} |W_{\mathbf{kq},\mathbf{p}}|^2 \int_{t_0}^t u^2(\tau - t_0) e^{-i[E_{\mathbf{p}_s}(\mathbf{p}) - E_{\mathbf{k}} - E_{\mathbf{q}}](t - \tau)} C_p(\tau) d\tau, \quad (6)$$

where $u(\tau - t_0)$ describes the dynamical effects of Ps leaving the surface. We have pointed out that Eq. (6) can also be derived from the quantum description of Ps formation.⁵ Here, we employ the classical trajectory approximation where $u(t)$ is an explicit function of $u(t) = e^{-at}$. Then Eq. (6) can be solved using a numerical calculation scheme similar to that of Sebastian and co-workers^{12,13} and Shindo and Kawai¹¹ in their ion-neutralization theories. However, in our Ps formation case, the calculation time is an order of magnitude longer than that of ion neutralization because of the final integration for \mathbf{p} .

The Ps fraction, or the total probability of Ps formation, is defined as follows:

$$f_{\mathbf{p}_s} = \sum_{\mathbf{p}} |C_p(\infty)|^2, \quad (7)$$

where $C_p(\infty)$ will be obtained from the solution of the integro-differential equation, (6). The energy and angular distribution, $w(v^2, \cos\theta)$ is defined by the following equation:

$$f_{\mathbf{p}_s} = \int d(v^2) \int d(\cos\theta) w(v^2, \cos\theta), \quad (8)$$

so that we can calculate $w(v^2, \cos\theta)$ from $C_p(t)$, which is obtained as a solution of Eq. (6).

In our previous theory of Ps formation, the wide-band approximation was used to solve Eq. (6) following the

$$f_{\mathbf{p}_s} = \sum_{\mathbf{p}} |C_p|^2 = 2\Delta_0 \int 6d^3p \int (dE_{\perp}/2\pi) f_-(E, T) (\pi/av_{\perp} \Delta_0) \text{sech}[\pi(E + E_{\mathbf{q}} - E_{\mathbf{p}_s} - p^2/4)/av_{\perp}], \quad (12)$$

where v_{\perp} is the final velocity of Ps perpendicular to the surface and $f_-(E, T)$ is the Fermi distribution for electrons.

As we see in Fig. 1, the integration of E_{\perp} is limited; the upper bound is derived by the existence of the Fermi sur-

face and the lower bound comes from the exclusion of energy gain by the time-dependent interaction,

$$\sum_{k_{\perp}} |W_{\mathbf{kq},\mathbf{p}}|^2 e^{iE_{\mathbf{k}}(t - \tau)} = 2\pi \int \rho'(E_{\perp}) \langle |W_{\mathbf{kq},\mathbf{p}}|^2 \rangle e^{iE(t - \tau)} dE_{\perp} / 2. \quad (9)$$

If we employ the wide-band approximation, where $\rho'(E_{\perp})$ and $\langle |W_{\mathbf{kq},\mathbf{p}}|^2 \rangle$ are assumed to be constant for E , Eq. (9) becomes

$$2\pi \int \rho'(E_{\perp}) \langle |W_{\mathbf{kq},\mathbf{p}}|^2 \rangle e^{iE(t - \tau)} dE_{\perp} / 2\pi = 2\pi \rho'(E_{\perp}^0) \langle |W_{\mathbf{kq},\mathbf{p}}|^2 \rangle \int e^{iE(t - \tau)} dE_{\perp} / 2\pi = 2\Delta_0 \delta(t - \tau). \quad (10)$$

In the second equality, we take the integration limits for E_{\perp} as $-\infty$ to ∞ : This is the wide-band approximation. Substituting (10) into Eq. (5) we obtain

$$i \frac{d}{dt} C_p(t) = \sum_{\mathbf{k}} V_{\mathbf{kq},\mathbf{p}} C_{\mathbf{k},\mathbf{q}}(t_0) - 2i\Delta_0 u^2(t - t_0) C_p(t). \quad (11)$$

We can solve it using the low-velocity approximation as follows:⁸

$$E_{\mathbf{k}} + E_{\mathbf{q}} - E_{\mathbf{p}_s} - p^2/4 \geq 0. \quad (13)$$

Therefore, Eq. (6) should be solved with the above bound

daries [see Fig. 2(a)]. However, in the wide-band approximation, the electron can go back to every state [see Fig. 2(b)]. Since Ps is very light, in contrast to the case of ion neutralization, it is impossible for positron neutralization. Thus the dissociation of Ps may be overestimated, which will be confirmed in the following numerical calculations.

Moreover, using the wide-band approximation, we cannot calculate Ps formation at the surfaces of narrow electron bands. As we see in Eq. (6), we use only the summation over k_{\perp} , and k_{\parallel} is restricted by p_{\parallel} . Thus, in contrast to the ion-neutralization case, we can calculate the Ps formation for any electronic band without the projection into the density of states.

III. RESULTS AND DISCUSSIONS

First we solve Eq. (6) numerically for a free-electron gas. We use a matrix element of the following form:

$$\begin{aligned} \pi\rho'(E_{\perp})\langle |W_{\mathbf{kq},\mathbf{p}}|^2 \rangle \\ = \begin{cases} \Delta_0 & (E_F - 2v_{\parallel}^2 \geq E_{\perp} \geq \phi_{\text{Ps}}^{+E_F} - (2v_{\parallel}^2 - v^2)), \\ 0 & \text{(otherwise)}, \end{cases} \end{aligned} \quad (14)$$

the above definition corresponding to the model of Fig. 2(a). To compare it with the wide-band model, Eq. (10), we assume that Δ_0 is constant. The difference between

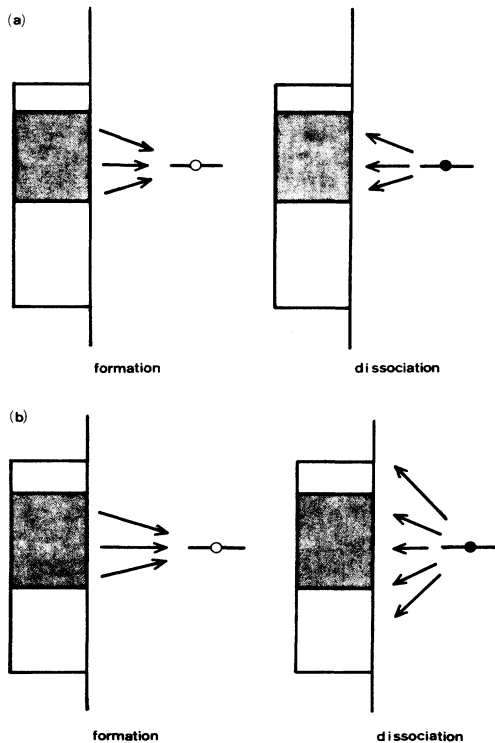


FIG. 2. (a) Schematic picture of the exact calculation. The band structure and Ps level are shown. The shaded part corresponds to the shaded part of Fig. 1. The arrow means the transition electron. (b) Schematic picture of the wide-band limit. In the dissociation process, the electron can transit to any level.

the model of Eq. (14) and the wide-band approximation for Ps is shown schematically in Fig. 2. In the model of Eq. (14), the level width, $\pi\rho'(e_{\perp})\langle |W_{\mathbf{kq},\mathbf{p}}|^2 \rangle$, is constant in the region where the energy and the momentum conservation hold. On the other hand, in the wide-band model, the level width is constant everywhere. The model of Eq. (14) is the simplest example of finite band width. Since the free-electron gas has a very simple structure, the above model will be a good approximation for simple metals.

We take $\phi_{\text{Ps}} = -0.095$ a.u., which corresponds to aluminum. Figure 3 shows the calculated energy distribution of angle-resolved Ps. θ is the ejection angle measured from the surface normal. On account of the dynamical factor $u(t)$, the distributions depend strongly on the ejection angle. Since the free-electron band has no fine structures, the curves in Fig. 3 are simple and structureless.

In Fig. 4 we show the angular distributions of the energy-resolved Ps for three different values of Δ_0 . The present results are quite different from the wide-band approximation (Fig. 5). For the case of $v^2 = 0.03$, the deviation comes from the overestimation of the dissociation

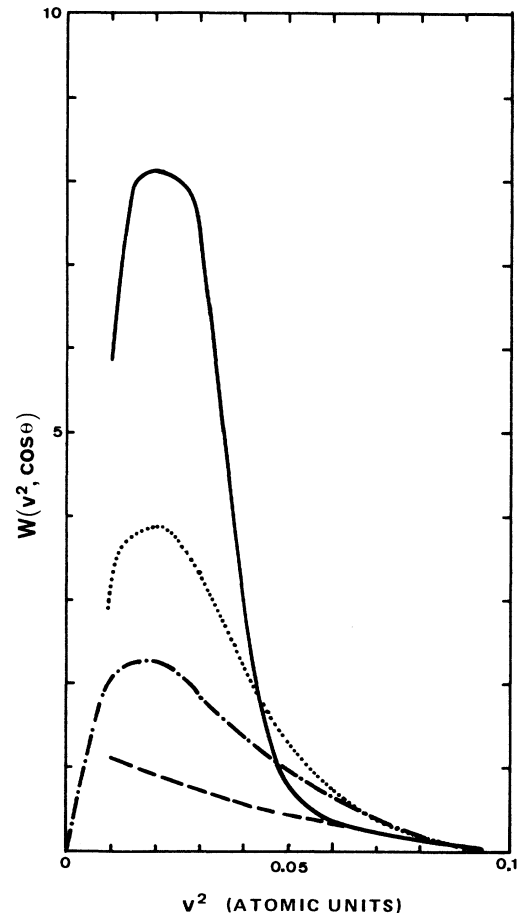


FIG. 3. Energy and angular distribution of Ps. $\Delta_0 = 0.09$. $\cos\theta = 0.2$ (solid line), 0.4 (dotted line), 0.6 (dashed-dotted line), and 1.0 (dashed line).

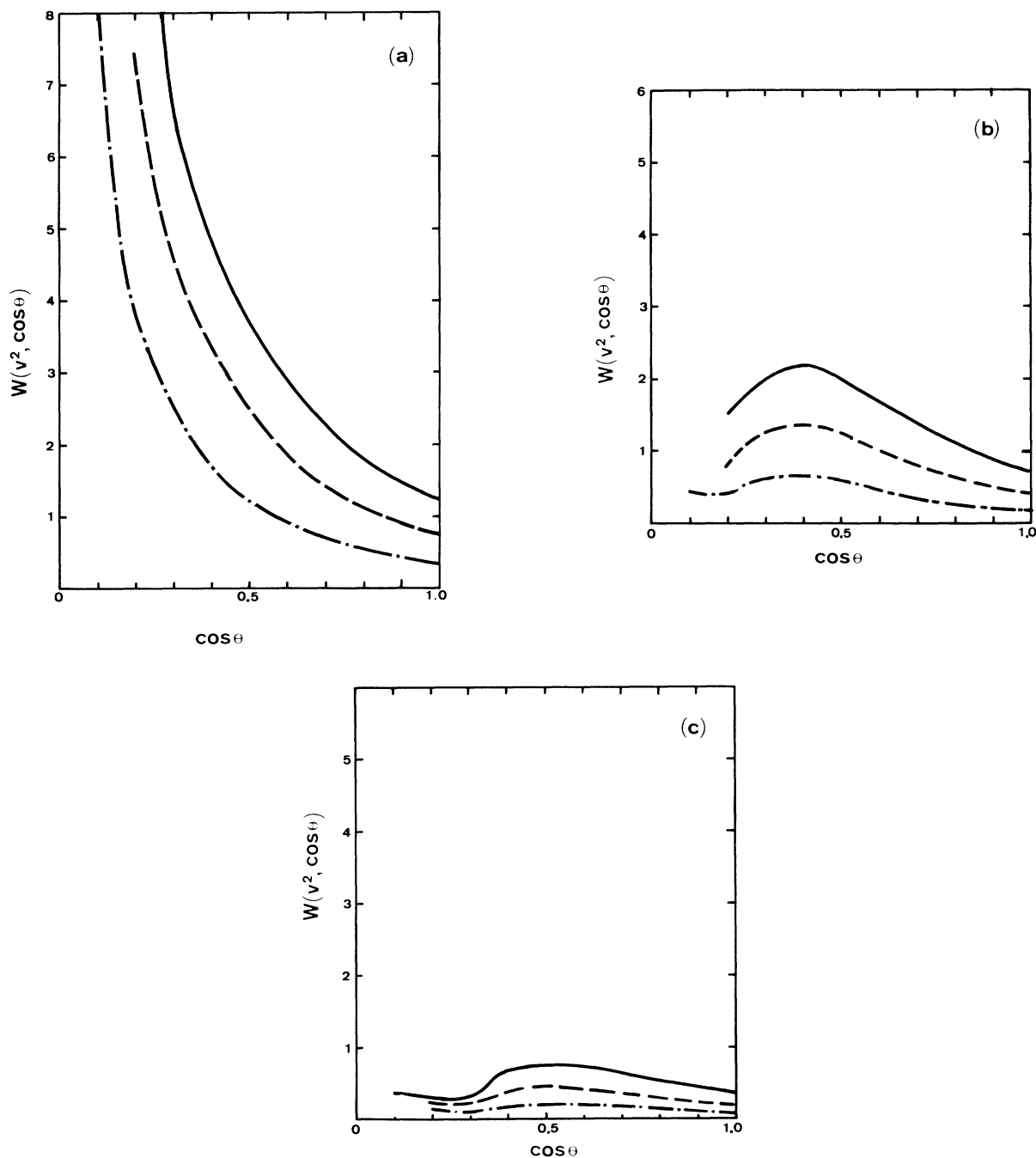


FIG. 4. Angular distribution of energy-resolved Ps flux. Three lines are $\Delta_0=0.04$ (dashed-dotted line), 0.09 (dashed line), and 0.16 (solid line). (a) $v^2=0.03$, (b) $v^2=0.05$, and (c) $v^2=0.07$.

rate of Ps in the wide-band approximation. The deviation is strong for small v . For $v^2=0.07$ the difference may come from both the wide-band approximation and the breakdown of the low-velocity approximation.⁶⁻⁸ Therefore, we should judge that the wide-band approximation of Eq. (12) is not adequate for Ps formation.

Next we calculate the Ps formation in the narrow-band case. If the band width is zero, the kinetic energy of emit-

ted Ps is fixed; $p^2/4=E_0-\phi_+-E_{Ps}$, where E_0 is the electronic energy level. Thus, if we calculate the Ps distribution of the above case using the golden rule, we will obtain a δ function for the Ps distribution. Therefore, in the case of narrow band, it is possible that the energy of the Ps formed is distributed from $p^2/4=E_a>0$ to $E_b<-\phi_{Ps}$, where E_a and E_b are energies corresponding to the bottom and the top of the band. A schematic picture of this

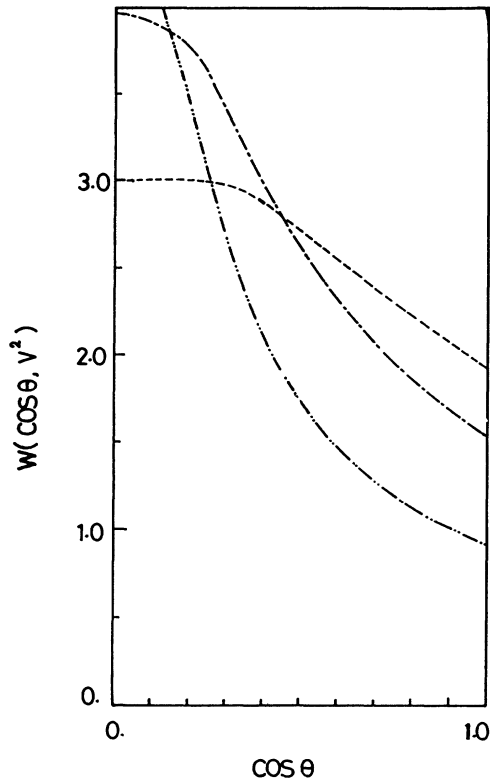


FIG. 5. Angular distribution of energy-resolved Ps flux from the calculation in the wide-band limit (Ref. 8). The three lines are $v^2=0.03$ (dashed line), $v^2=0.05$ (dashed-dotted line), and $v^2=0.07$ (dashed-double-dotted line).

is shown in Fig. 6 as a relation between the density of states of surface electrons and the Ps distribution for a certain emission angle of Ps. In Fig. 6, the left-handed graph is the one-dimensional density for states of surface electrons for the emission angle of Ps, and the right-handed graph is the rough estimation of the corresponding Ps distribution from the golden-rule formula. The normal axis is the surface-normal energy of an electron-positron pair for the emission angle of Ps. Here we assume a simple spherical narrow band of the form

$$E(k) = E_0 + E_1 \cos(bk) . \quad (15)$$

We perform the calculation for three cases. (a) The width of the filled part of the band is nearly equal to $-\phi_{Ps}$:

$$E_0 = -\phi_-, \quad E_1 = -0.1, \quad b = 0.5 .$$

(b) The width of the filled part of the band is narrow compared with $-\phi_{Ps}$:

$$E_0 = -\phi_-, \quad E_1 = -0.05, \quad b = 0.5 .$$

(c) The width of the filled part of the band is narrow compared with $-\phi_{Ps}$:

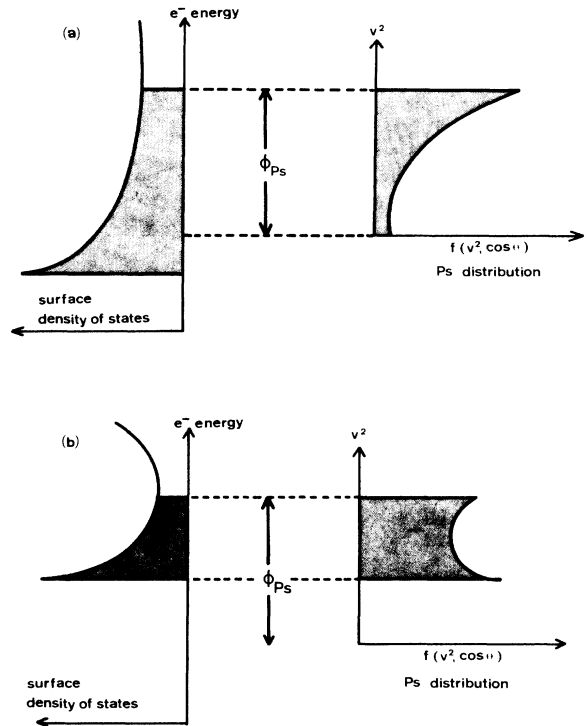


FIG. 6. Schematic picture of the band structure and the corresponding angle-resolved Ps energy distribution based on the ordinary golden rule. (a) The width of the filled part of the band is nearly equal to $-\phi_{Ps}$. (b) The width of the filled part of the band is narrow in comparison with $-\phi_{Ps}$.

$$E_0 = -\phi_-, \quad E_1 = -0.05, \quad b = 0.2 ,$$

where $-\phi_{Ps} = 0.095$. Case (a) is shown in Fig. 6 (a) and cases (b) and (c) in Fig. 6 (b), respectively. In case (a), the width of the filled part of the band is nearly equal to $-\phi_{Ps}$. For cases (b) and (c), the width of the filled part of the band is nearly half of $-\phi_{Ps}$, so that, as we see in Fig. 6(b), the simple golden rule of Eq. (1) predicts that the Ps energy is distributed only from $v^2 = 0.045$ to 0.095 . Thus, we would not observe Ps of kinetic energy v^2 , less than 0.045 , if we employed the golden-rule formula, as we see in Fig. 6(b). The difference between (b) and (c) is only the value of b .

In Fig. 7, we show the calculated energy distribution of angle-resolved Ps for the above three cases. In Fig. 7(a) we find that the energy distribution is much different from that for the free-electron band of Fig. 3. This seems strange because the width of the filled part of the band is larger than $-\phi_{Ps}$ in both cases. This difference comes from the band structure. Thus, we can read the band structures from the angle- and energy-resolved Ps distributions.

From Figs. 7(b) and 7(c), we find that the value is distributed from $v^2 = 0$ to 0.095 , which contradicts the prediction of the simple golden rule. This comes from the

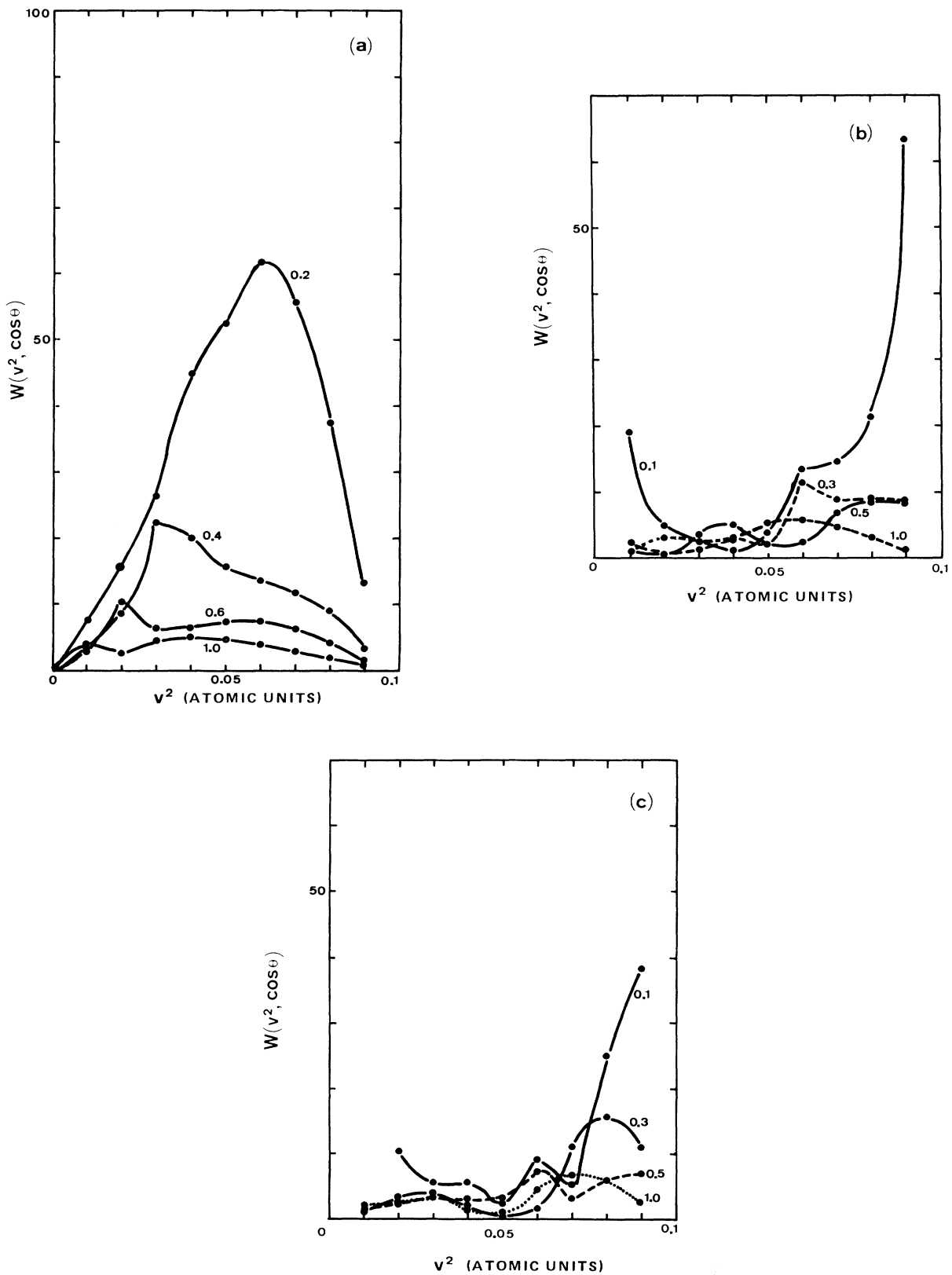


FIG. 7. Energy distribution of angle-resolved Ps flux. The value of $\cos\theta$ is shown in each figure. (a) Case (a); (b) case (b); (c) case (c). The numerical calculation is only done at the point of the dots on the graphs.

dynamical interaction. In contrast to a static-interaction model (golden-rule formula), the correlation time of the dynamical interaction is restricted by the lifetime of the Ps level due to the dissociation of Ps (different from the lifetime of 2γ decay). The finite interaction time causes the energy loss of Ps due to the Heisenberg broadening of the energy level. The loss energy corresponds to the excitation of the electron system in the solid. From the calculated results in Figs. 7(b) and 7(c), we find that the energy-loss process due to the Heisenberg broadening of the Ps level is important for describing the energy distribution of Ps. Here, we should recall, Eq. (13), that we exclude the energy gain due to the Heisenberg broadening in contrast to the ion neutralization, because metal surfaces cannot supply energy to Ps via Heisenberg uncertainty. The energy distribution is mainly weighted on the high-energy side because of the band structure. It is the reflection of the surface density of state smeared out by the dynamical interaction.

The distributions of Figs. 7(b) and 7(c) oscillate in energy or velocity. This may correspond to the quasisonant oscillation which is found in ion neutralization,¹⁰ since the dispersion of the bands is very flat.

In Fig. 8 we show the angular distribution of energy-integrated Ps. The distribution profiles are very different from each other. The distribution for a free-electron band [Fig. 8(a)] is a simple curve. The distribution for the narrow band of case (a) increases with decreasing $\cos\theta$. The distribution of cases (b) and (c) is very flat compared with the case (a) and the free-electron-band case. The curvature decreases with decreasing surface-electron-band dispersion. If surface electron has no dispersion relation, it is clear that the angular distribution is restricted only by the matrix element. The result of numerical calculations agrees with the above considerations.

IV. CONCLUSION

We have found that the wide-band approximation, which has been used in ion neutralization, is not adequate for Ps formation. From the calculated distributions for several types of bands, it was found that the Ps distribution is very sensitive to the band structure of surface electrons. Therefore, we conclude that PsFS measurement can be used as a sensitive probe to determine surface electronic band structures. A further theoretical problem is how one quantizes the trajectory of Ps.⁵

ACKNOWLEDGMENTS

We are grateful to Professor Y. H. Ohtsuki, Professor S. Tanigawa, and Dr. M. Kato for their valuable discussions. We also thank Professor M. Tsukada, Dr. N. Shima, and the members of their group at Tokyo University

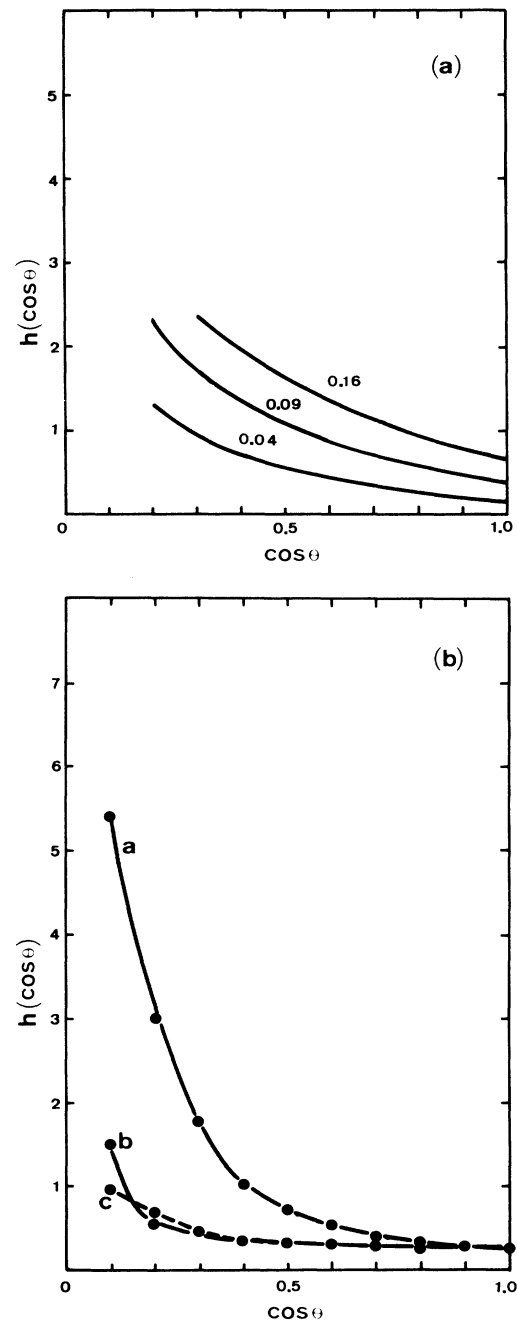


FIG. 8. Angular distribution of Ps flux. (a) Electron-gas model. The three lines are $\Delta_0=0.04, 0.09,$ and $0.16,$ respectively. (b) Narrow band model. The three lines are cases (a), (b), and (c) in the text, respectively.

for discussions. This work is supported by the Japan Society for the Promotion of Science and a Grant-in-Aid for Science Research from the Ministry of Education of Japan.

- *The author has changed the spelling of his name from "Isii" to "Ishii."
- ¹A. Held and S. Kahana, *Can. J. Phys.* **42**, 1908 (1964).
- ²H. Kanazawa, Y. H. Ohtsuki, and S. Yanagawa, *Phys. Rev.* **138**, A1155 (1965).
- ³J. B. Pendry, in *Positron Solid-State Physics*, edited by W. Brandt and A. Dupasquier (North-Holland, Amsterdam, 1983).
- ⁴A. P. Mills, Jr., L. Pfeiffer, and P. M. Platzman, *Phys. Rev. Lett.* **51**, 1085 (1983).
- ⁵S. Shindo and A. Ishii (unpublished).
- ⁶A. Isii, *Surf. Sci.* **147**, 277 (1984).
- ⁷A. Isii, *Surf. Sci.* **147**, 295 (1984).
- ⁸A. Isii (unpublished).
- ⁹R. M. Nieminen and J. Oliva, *Phys. Rev. B* **22**, 2226 (1980).
- ¹⁰W. Bloss and D. Hone, *Surf. Sci.* **72**, 277 (1978).
- ¹¹S. Shindo and R. Kawai, *Surf. Sci.* **165**, 477 (1986).
- ¹²K. L. Sebastian, V. C. Jyothi Basu, and T. R. Grimley, *Surf. Sci.* **110**, L571 (1981).
- ¹³T. R. Grimley, V. C. Jyothi Basu, and K. L. Sebastian, *Surf. Sci.* **124**, 305 (1983).
- ¹⁴R. Brako and D. M. Newns, *Surf. Sci.* **108**, 253 (1981).
- ¹⁵J. N. M. Van Wunnik, R. Brako, K. Makoshi, and D. M. Newns, *Surf. Sci.* **126**, 618 (1983).
- ¹⁶M. Tsukada and N. Shima, in *Dynamical Processes and Ordering on Solid Surfaces*, edited by A. Yoshimori and M. Tsukada (Springer-Verlag, Berlin, 1985).
- ¹⁷Z. L. Miskovic and R. K. Janev, *Surf. Sci.* **166**, 480 (1986).

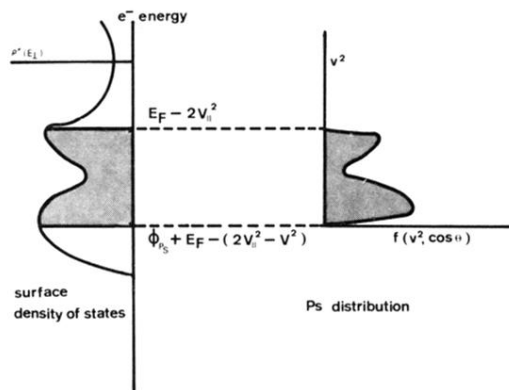


FIG. 1. Schematic picture of PsFS. The left graph is the one-dimensional density of states for surface electrons. The right graph is the corresponding Ps energy distribution. The lower limit and the upper limit of the Ps distribution is discussed in Sec. II. The distribution has a similar profile as that of the surface density of states. Here, v^2 is the kinetic energy of Ps in atomic units.

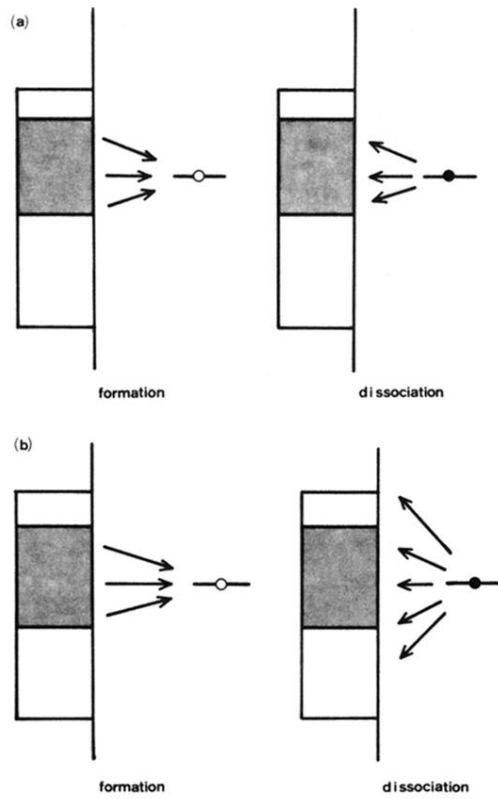


FIG. 2. (a) Schematic picture of the exact calculation. The band structure and Ps level are shown. The shaded part corresponds to the shaded part of Fig. 1. The arrow means the transition electron. (b) Schematic picture of the wide-band limit. In the dissociation process, the electron can transit to any level.

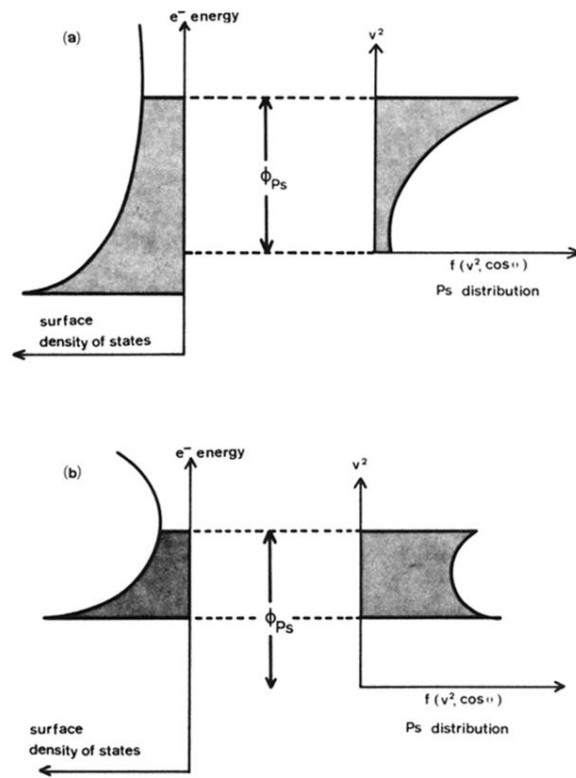


FIG. 6. Schematic picture of the band structure and the corresponding angle-resolved Ps energy distribution based on the ordinary golden rule. (a) The width of the filled part of the band is nearly equal to $-\phi_{Ps}$. (b) The width of the filled part of the band is narrow in comparison with $-\phi_{Ps}$.